IEEE Robotics and Automation Letters (RAL) paper presented at the
2020 IEEE International Conference on Robotics and Automation (ICRA)
31 May - 31 August, 2020. Paris, France

Time Optimal Motion Planning and Admittance Control for Cooperative Grasping

D. Kaserer[1], H. Gattringer[2], A. Müller[2]

***Abstract*— Cooperative grasping refers to the situation when an object is manipulated by multiple robots and the grasp is achieved by the unilateral contact between the robots and the object. This is different from the cooperation of multiple robots where each robot rigidly grasps the object. Motion planning of cooperative grasping tasks involves active force control of the interaction wrench in order to ensure stable grasp. This becomes particularly challenging when aiming at time optimal motions. It is crucial that the trajectories are continuous up to third-order, in order to satisfy velocity, acceleration, and jerk as well as torque limits of the robots. A solution approach is presented for the time optimal path following of two robots performing cooperative grasping tasks. The time optimal path is determined with a dynamic programing method. An admittance control scheme in task space is proposed and used to generate the contact wrench. The method is applicable to grasping of general objects that are in surface contact with the robot.**

***Index Terms*— Grasping, collaboration, admittance control, motion planning, optimal control, dynamic programing, impact**

I. Introduction

In various situations it is desirable to enable two robots to cooperatively lift and manipulate an object which is too heavy for either of the robots, while it is economically not viable to implement another robot with sufficiently larger payload. Yet the handling task should be performed in minimal time. This is addresses in this paper.

The cooperation of multiple robots where each robot rigidly grasps an object has been a research topic for many years. Since in such scenarios the robots form a (or multiple) kinematic loop, hybrid force-position control schemes are frequently used [6], [15]. For the particular case of a dual-arm systems it was proposed that one robot is force controlled while the second robot is position controlled [1], so that the first follows the motion of the second.

The problem of cooperative grasping with a dual arm setup has been recently addressed in [4], where both robots are impedance controlled. Also the cooperative grasping of flexible objects was addressed in [23], [22]. An overview on dual arm manipulation can be found in [20]. A time optimal motion planning and control scheme for dual arm systems is to the authors best knowledge not reported up to now.

In this paper, the collaborative manipulation of an object is pursued with a *cooperative grasp*. A cooperative grasp of two robots will be understood as the force closure of an object due to the unilateral contact with two robots. This is to be distinguished from the cooperation of two robots where an object is rigidly grasped by each individual robot (with a gripper). In a cooperative grasping scenario the individual robots can be thought of as the fingers of an ordinary gripper.

In this paper the time optimal motion of two non-redundant 6DOF serial robots performing a cooperative grasp is addressed. The motion planing must ensure a sufficient contact wrench, and take into account the friction properties of the contact as well as the object dynamics, in order to ensure 'cooperative force closure' (rather than force closure within a gripper). To this end, in this paper, a time optimal motion planning problem is formulated that accounts for the dynamics of the cooperating robots and for the force closure (friction cone constraints). This is solved with a dynamic programming method [10] taking into account jerk limits. An admittance control scheme is used to generate the so-determined dynamic grasp wrenches. That is, both robots are admittance controlled, instead of one position and the other force controlled, for instance. The grasp wrench is achieved by a prescribed virtual penetration of the object. Experimental results are shown to enable high-speed collaborative grasping. Initial results for admittance control of two collaborating robots where time-optimal motion is not considered were reported in [7].

This paper deals with time optimal path following, i.e. the path of the object in workspace is given. The path planning is not the topic of this paper. A recent overview of multi-arm motion planning can be found in [14]. It is presumed throughout the paper that 1) the external loads only act on the EE, and 2) measurement of these EE wrenches is available. These assumption can be easily lifted, but this is not necessary for the addressed application.

II. Dynamic Model of Serial Manipulators

A serial n DOF robotic manipulator is considered. At the terminal body n an EE is attached at which an EE frame is defined. The EE pose is described by the position vector $\mathbf{r}_{\mathrm{E}}$ to the origin of the EE frame expressed in the world-fixed inertial frame, and by the rotation matrix $\mathbf{R}_{\mathrm{E}}$ of the EE relative to the inertia frame, summarized as $\mathbf{z}_{\mathrm{E}} = (\mathbf{r}_{\mathrm{E}}, \mathbf{R}_{\mathrm{IE}})$. The EE twist is represented by the vector $\mathbf{V}_{\mathrm{IE}} = (\mathbf{v}_{\mathrm{E}}, \boldsymbol{\omega}_{\mathrm{E}}) \in \mathbb{R}^6$. Denote with $\mathbf{q} \in \mathbb{V}^n$ the vector of n joint variables.

The solution to the geometric forward kinematics problem is given as $\mathbf{z}_{\mathrm{E}} = f(\mathbf{q})$, with the geometric forward kinematic mapping $f : \mathbb{V}^n \rightarrow SE(3)$. The velocity forward kinematics problem at a configuration $\mathbf{q}$ is given by $\mathbf{V}_{\mathrm{E}} = \mathbf{J}(\mathbf{q})\dot{\mathbf{q}}$, where $\mathbf{J}(\mathbf{q})$ is the $d \times n$ forward kinematics Jacobian (assumed non-singular). The EE DOF is $d \leq n$. In this paper

[1]B&R Industrial Automation, Eggelsberg, Austria dominik.kaserer@br-automation.com
[2]Institute of Robotics, Johannes Kepler University Linz, Austria {hubert.gattringer,a.mueller}@jku.at

kinematically non-redundant spatial 6 DOF manipulators are considered, i.e. $d = n = 6$.

The equations of motion (EOM) of a serial robot are written as

$$\mathbf{M}(\mathbf{q})\,\ddot{\mathbf{q}} + \mathbf{g}(\dot{\mathbf{q}}, \mathbf{q}) = \mathbf{Q} - \mathbf{Q}_{\mathrm{E}} \tag{1}$$

where $\mathbf{M}$ is the generalized mass matrix, $\mathbf{g}$ represents Coriolis, centrifugal, and all other generalized forces, $\mathbf{Q}$ is the vector of generalized driving forces, and $\mathbf{Q}_{\mathrm{E}}$ generalized forces due to loads at the EE. The generalized driving forces are determined by the motor torques/forces $\boldsymbol{\tau} \in \mathbb{R}^n$ as $\mathbf{Q} := \boldsymbol{B}\boldsymbol{\tau}$, with $\mathbf{B} := \mathrm{diag}(i_1, \ldots, i_n)$ given in terms of the gear ratios i_j of the motors $j = 1, \ldots, n$.

Denote with $\mathbf{h}_{\mathrm{E}} = (\mathbf{f}_{\mathrm{E}}, \mathbf{m}_{\mathrm{E}}) \in se^*(3)$ the wrench due to external loads at the EE. It is assumed that external loads only act at the EE, so that the corresponding generalized forces are $\mathbf{Q}_{\mathrm{E}} := \mathbf{J}^T \mathbf{h}_{\mathrm{E}}$. Generally, arbitrary external loads, not necessarily acting at the EE, can be taken into account [5], [9], [12], which is not pursued in this paper.

If the geometric path of the robot is known, then the joint coordinate vector $\mathbf{q}$ can be expressed in terms of a path parameter s. Its time evolution $s(t)$ is determined according to a specific goal. In this paper the time optimal motion is addressed. The speed along the path is $\dot{s}(s)$. It is beneficial to introduce $z(s) := \dot{s}(s)^2$. With a path parameterization $\mathbf{q}(s)$, the joint velocity, acceleration, and jerk are given in terms of the derivatives w.r.t. the path parameter, denoted by $()'$, and the 'path speed' $\dot{s}$

$$\dot{\mathbf{q}} = \mathbf{q}'\sqrt{z}, \ddot{\mathbf{q}} = \mathbf{q}''z + \frac{1}{2}\mathbf{q}'z', \dddot{\mathbf{q}} = \left(\mathbf{q}'''z + \frac{3}{2}\mathbf{q}''z' + \frac{1}{2}\mathbf{q}'z''\right)\sqrt{z}. \tag{2}$$

Introducing these into the EOM (1) yields [18]

$$\mathbf{a}(s)\,z' + \mathbf{b}(s)\,z + \mathbf{c}(s) + \mathbf{d}(s)\sqrt{z} = \mathbf{Q} - \mathbf{Q}_{\mathrm{E}}, \tag{3}$$

where the identity $\ddot{s} = 1/2z'$ is used. While such a formulation is usually used for trajectory planning, the formulation (3) is particular since it contains the term $\mathbf{d}\sqrt{z}$. This terms represents the effect of viscous friction, and is hence crucial for highly dynamic application and time optimal motion in particular.

The EOM can be transformed to task space coordinates, see e.g. [11]. Substituting the acceleration, yields (for non-redundant robots)

$$\boldsymbol{\Lambda}(\mathbf{q})\dot{\mathbf{V}}_{\mathrm{E}} + \mathbf{J}^{-T}(\mathbf{q})\,\mathbf{g}(\dot{\mathbf{q}}, \mathbf{q}) - \boldsymbol{\Lambda}\dot{\mathbf{J}}(\mathbf{q}, \dot{\mathbf{q}})\,\dot{\mathbf{q}} = \mathbf{J}^{-T}\mathbf{Q} - \mathbf{h}_{\mathrm{E}} \tag{4}$$

where

$$\boldsymbol{\Lambda} := \mathbf{J}^{-T}\mathbf{M}\mathbf{J}^{-1} \tag{5}$$

is the task space mass matrix collocated at the EE. The final task space formulation of the EOM is obtained by replacing $\dot{\mathbf{q}}$ with $\dot{\mathbf{q}} = \mathbf{J}^{-1}\mathbf{V}_{\mathrm{E}}$. This is not required in the following.

III. Admittance Control of Non-Redundant Robots in Task Space

The admittance control scheme introduced in [9], [8] is adapted to this problem. Admittance control is preferred since it is well known that impedance control may not lead to a desired impedance due to parameter uncertainties and Coulomb friction in particular [3]. Denote with $\mathbf{q}_{\mathrm{d}}(t)$ the joint trajectory according to a desired task $\mathbf{z}_{\mathrm{E,d}}$, which is e.g. determined via inverse kinematics or optimal motion planning (as in section V.B). The aim of an admittance control scheme (also called indirect impedance control) is to achieve a (controlled) compliance, i.e. generating an evasive motion (a deviation from $\mathbf{q}_{\mathrm{d}}$) of the robot as a reaction to an external force/torque. The joint trajectory corresponding to this compliant motion is denoted with $\mathbf{q}_{\mathrm{c}}(t)$ so that $\Delta\mathbf{q} := \mathbf{q}_{\mathrm{d}} - \mathbf{q}_{\mathrm{c}}$ is the deviation from a desired motion. Admittance control requires an estimate of the external load $\mathbf{h}_{\mathrm{E}}$. It is assumed in the following that such an estimate is available. Most reliable is the direct force/torque measurement at the EE. A momentum based observer was used to this end in [9].

According to a desired admittance and EE load $\mathbf{h}_{\mathrm{E}}$, the EE trajectory must be controlled so to deviate from the desired trajectory $\mathbf{z}_{\mathrm{E,d}}$. Denote the deviation of the EE pose from its desired value with $\Delta\mathbf{z}_{\mathrm{E}}^T := \left((\mathbf{r}_{\mathrm{E,d}} - \mathbf{r}_{\mathrm{E}})^T, (\log(\mathbf{R}_{\mathrm{IE,d}}\mathbf{R}_{\mathrm{IE}}^T)^T\right)$, the deviation of the EE velocity with $\Delta\mathbf{V}_{\mathrm{E}}^T = (\mathbf{v}_{\mathrm{E,d}}^T - \mathbf{v}_{\mathrm{E}}^T, \boldsymbol{\omega}_{\mathrm{E,d}}^T - \boldsymbol{\omega}_{\mathrm{E}}^T)$, and with $\Delta\dot{\mathbf{V}}_{\mathrm{E,d}}$ that of the acceleration.

The desired EE dynamics in task space is described by

$$\mathbf{M}_{\mathrm{E}}\Delta\dot{\mathbf{V}}_{\mathrm{E}} + \mathbf{D}_{\mathrm{E}}\Delta\mathbf{V}_{\mathrm{E}} + \mathbf{K}_{\mathrm{E}}\Delta\mathbf{z}_{\mathrm{E}} = \mathbf{h}_{\mathrm{E}} \tag{6}$$

where $\mathbf{M}_{\mathrm{E}}, \mathbf{D}_{\mathrm{E}}$, and $\mathbf{K}_{\mathrm{E}}$ are the mass, damping, and stiffness matrix, respectively, according to the desired admittance of the robot at the EE.

The new admittance control law can be introduced starting from the impedance control [9] in task space. To this end, the joint accelerations $\ddot{\mathbf{q}}$ are used as control inputs

$$\mathbf{w} := \ddot{\mathbf{q}} \tag{7}$$

so that the drive torques follow from (1) as

$$\mathbf{Q} = \mathbf{M}(\mathbf{q})\mathbf{w} + \mathbf{g}(\mathbf{q}, \dot{\mathbf{q}}) - \mathbf{Q}_{\mathrm{E}}. \tag{8}$$

The following control is used for the inputs $\mathbf{w}$

$$\mathbf{w} = \mathbf{J}^{-1}\left(\mathbf{M}_{\mathrm{E}}^{-1}\left(\mathbf{D}_{\mathrm{E}}\Delta\mathbf{V}_{\mathrm{E}} + \mathbf{K}_{\mathrm{E}}\Delta\mathbf{z}_{\mathrm{E}} - \mathbf{h}_{\mathrm{E}}\right) + \dot{\mathbf{V}}_{\mathrm{E,d}} - \dot{\mathbf{J}}\dot{\mathbf{q}}\right). \tag{9}$$

Setting $\ddot{\mathbf{q}} = \mathbf{w}$, and premultiplying (9) with $\mathbf{M}_E\mathbf{J}$ yields (6). Thus the control law (9) leads to the desired admittance.

With control inputs (7), the control scheme (9) relies on perfect tracking of the desired position $\mathbf{q} = \mathbf{q}_{\mathrm{c}}$. That is, the admittance control attains a cascaded structure (Fig. 1) consisting of position control and subsequent compliance control (9). A high gain PD-controller in combination with a feed forward term, computed from the inverse dynamics of (1) for desired values $\mathbf{q}_{\mathrm{c}}, \dot{\mathbf{q}}_{\mathrm{c}}, \ddot{\mathbf{q}}_{\mathrm{c}}$, is used for position control. The desired acceleration $\ddot{\mathbf{q}}_{\mathrm{c}}$, used as input (7) for the position control, is computed as

$$\ddot{\mathbf{q}}_{\mathrm{c}} = \mathbf{J}^{-1}\left(\mathbf{M}_{\mathrm{E}}^{-1}\left(\mathbf{D}_{\mathrm{E}}\Delta\mathbf{V}_{\mathrm{E}} + \mathbf{K}_{\mathrm{E}}\Delta\mathbf{z}_{\mathrm{E}} - \mathbf{h}_{\mathrm{E}}\right) + \dot{\mathbf{V}}_{\mathrm{E,d}} - \dot{\mathbf{J}}\dot{\mathbf{q}}_{\mathrm{c}}\right) \tag{10}$$

similarly to impedance control. Joint velocities $\dot{\mathbf{q}}_{\mathrm{c}}$ and positions $\mathbf{q}_{\mathrm{c}}$ are calculated by integration of (10). It should be remarked that for a kinematically redundant manipulator it is possible to define a desired admittance in task space and in joint space, where the EE admittance has first priority and the null space admittance has second priority [9].

IV. Admittance Control of Cooperating Robots

A. Grasp Kinetostatics

The object is grasped (perfect force closure) by the two robots at two distinct locations (Fig. 2). The grasp geometry is described relative to the COM S of the manipulated object. Denote with $\mathbf{r}_{\mathrm{SE1}}$ and $\mathbf{r}_{\mathrm{SE2}}$ the position vector from the COM S to the grasp point of robot 1 and 2, respectively, both expressed in the inertial frame. The EE wrenches $\mathbf{h}_{\mathrm{E1}} = \left(\mathbf{f}_{\mathrm{E1}}^T, \mathbf{m}_{\mathrm{E1}}^T\right)^T$ and $\mathbf{h}_{\mathrm{E2}} = \left(\mathbf{f}_{\mathrm{E2}}^T, \mathbf{m}_{\mathrm{E2}}^T\right)^T$, are measure at the respective EE. They are summarized in the vector $\mathbf{h}_{\mathrm{E12}} = \left(\mathbf{h}_{\mathrm{E1}}^T, \mathbf{h}_{\mathrm{E2}}^T\right)^T \in \mathbb{R}^{12}$. The net wrench $\mathbf{h}_{\mathrm{S}} = \left(\mathbf{f}_{\mathrm{S}}^T, \mathbf{m}_{\mathrm{S}}^T\right)^T$ generated at the COM S is determined as

$$\mathbf{h}_{\mathrm{S}} = \mathbf{W}\mathbf{h}_{\mathrm{E12}}, \text{ with } \mathbf{W} := \begin{pmatrix} \mathbf{I} & \mathbf{0} & \mathbf{I} & \mathbf{0} \\ \widetilde{\mathbf{r}}_{\mathrm{SE1}} & \mathbf{I} & \widetilde{\mathbf{r}}_{\mathrm{SE2}} & \mathbf{I} \end{pmatrix} \tag{11}$$

where $\mathbf{W}$ is the 6×12 grasp matrix. The net wrench $\mathbf{h}_{\mathrm{S}}$ will be used to move the object, whereas the actual grasp wrench holding the object is the component of $\mathbf{h}_{\mathrm{E12}}$ in the null-space of the grasp matrix. Given a desired net wrench $\mathbf{h}_{\mathrm{S}}$, the necessary EE wrenches can be determined as

$$\mathbf{h}_{\mathrm{E12}} = \mathbf{W}^{\#}\mathbf{h}_{\mathrm{S}} + \mathbf{V}\mathbf{h}_{\mathrm{I}} \tag{12}$$

where $\mathbf{W}^{\#} = \mathbf{G}\mathbf{W}^T(\mathbf{W}\mathbf{G}\mathbf{W}^T)^{-1}$ is a $\mathbf{G}$-weighted pseudoinverse, and $\mathbf{V} \in \mathbb{R}^{12,6}$ is an orthogonal complement matrix such that $\mathbf{W}\mathbf{V} = \mathbf{0}$. The $\mathbf{h}_{\mathrm{I}} \in \mathbb{R}^6$ is a desired grasp wrench that generates internal prestressing. The weighting matrix must be chosen so to ensure that $\mathbf{W}^{\#}\mathbf{h}_{\mathrm{S}}$ does not generate null-space components. It was shown in [24] that

$$\mathbf{G} = \begin{pmatrix} \mathbf{0} & \mathbf{I} & \mathbf{0} & \mathbf{0} \\ \mathbf{I} & \mathbf{0} & \mathbf{0} & \mathbf{0} \\ \mathbf{0} & \mathbf{0} & \mathbf{0} & \mathbf{I} \\ \mathbf{0} & \mathbf{0} & \mathbf{I} & \mathbf{0} \end{pmatrix}, \mathbf{W}^{\#} = \begin{pmatrix} \frac{1}{2}\mathbf{I} & \mathbf{0} \\ -\frac{1}{2}\widetilde{\mathbf{r}}_{\mathrm{SE1}} & \frac{1}{2}\mathbf{I} \\ \frac{1}{2}\mathbf{I} & \mathbf{0} \\ -\frac{1}{2}\widetilde{\mathbf{r}}_{\mathrm{SE2}} & \frac{1}{2}\mathbf{I} \end{pmatrix} \tag{13}$$

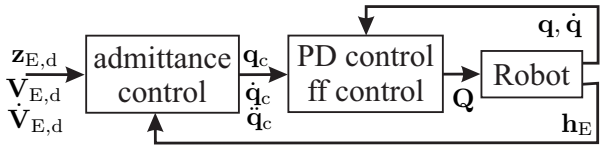

Fig. 1. Admittance control scheme.

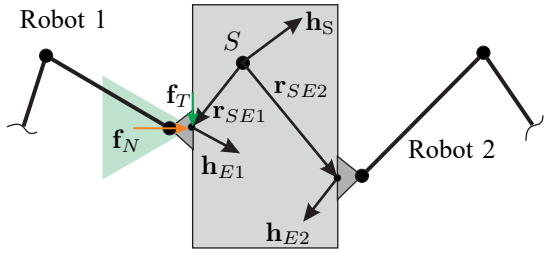

Fig. 2. Grasp kinematics and wrenches of a collaborative grasp.

do not lead to internal grasp wrenches. Also the orthogonal complement is not unique. Following [19], the matrices

$$\mathbf{V} = \begin{pmatrix} -\mathbf{I} & \mathbf{0} \\ \widetilde{\mathbf{r}}_{\mathrm{SE1}} & -\mathbf{I} \\ \mathbf{I} & \mathbf{0} \\ -\widetilde{\mathbf{r}}_{\mathrm{SE2}} & \mathbf{I} \end{pmatrix}, \mathbf{V}^{\#} = \frac{1}{2}\begin{pmatrix} -\mathbf{I} & \mathbf{0} & \mathbf{I} & \mathbf{0} \\ -\widetilde{\mathbf{r}}_{\mathrm{SE1}} & -\mathbf{I} & \widetilde{\mathbf{r}}_{\mathrm{SE2}} & \mathbf{I} \end{pmatrix} \tag{14}$$

will be used.

B. Object Kinematics and Dynamics

The EE wrenches are related to the net wrench $\mathbf{h}_{\mathrm{S}}$ acting on the object by (12). The latter is determined by the motion of the manipulated object. The Newton-Euler equations are used to compute the wrench necessary to achieve a prescribed motion. When the object is grasped, the pose of the object is known from the EE poses, i.e. from the state of the two robots. It will be assumed that the EE locations at the object are known. It is further assumed that the grasp geometry is constant as long as the object is grasped, i.e. no slipping of the object.

The pose of the object is described by the position vector $\mathbf{r}_{\mathrm{S}}$ of its COM, and its orientation relative to the world-fixed inertial frame by a rotation matrix $\mathbf{R}_{\mathrm{IS}}$. The motion of the object is prescribed by a curve parameter $s(t)$

$$\mathbf{r}_{\mathrm{S}}(t) = \mathbf{r}_{\mathrm{S}}(s(t)) \text{ and } \mathbf{R}_{\mathrm{IS}}(t) = \mathbf{R}_{\mathrm{IS}}(s(t)). \tag{15}$$

The translational and angular velocity and acceleration are

$$\begin{aligned} \dot{\mathbf{r}}_{\mathrm{S}} &= \mathbf{r}_{\mathrm{S}}'(s)\sqrt{z}, \ \ddot{\mathbf{r}}_{\mathrm{S}} = \mathbf{r}_{\mathrm{S}}''(s)z + \frac{1}{2}\mathbf{r}_{\mathrm{S}}'(s)z' \\ \boldsymbol{\omega}_{\mathrm{S}} &= \boldsymbol{\omega}_{\mathrm{S}}(s)\sqrt{z}, \ \dot{\boldsymbol{\omega}}_{\mathrm{S}} = \boldsymbol{\omega}_{\mathrm{S}}'(s)z + \frac{1}{2}\boldsymbol{\omega}_{\mathrm{S}}(s)z'. \end{aligned} \tag{16}$$

Denote with $\mathbf{f}_{\mathrm{S}}$ and $\mathbf{m}_{\mathrm{S}}$ respectively the force and torque acting at the COM of the object. The object dynamics is governed by the Newton-Euler equations

$$\begin{aligned} m(\ddot{\mathbf{r}}_{\mathrm{S}} + \mathbf{g}) &= \mathbf{f}_{\mathrm{S}} \\ (\boldsymbol{\Theta}_{\mathrm{S}}\dot{\boldsymbol{\omega}}_{\mathrm{S}} + \widetilde{\boldsymbol{\omega}}_{\mathrm{S}}\boldsymbol{\Theta}_{\mathrm{S}}\boldsymbol{\omega}_{\mathrm{S}}) &= \mathbf{m}_{\mathrm{S}} \end{aligned} \tag{17}$$

where m is the mass, $\boldsymbol{\Theta}_{\mathrm{S}}$ the inertia tensor w.r.t. the COM, and $\mathbf{g}$ the vector of gravitational acceleration. This can be written in terms of curve parameter and the wrench (11) as

$$\frac{1}{2}\underbrace{\begin{pmatrix} m\mathbf{r}_{\mathrm{S}}' \\ \boldsymbol{\Theta}_{\mathrm{S}}\boldsymbol{\omega}_{\mathrm{S}} \end{pmatrix}}_{\mathbf{a}_{\mathrm{S}}(s)} z' + \underbrace{\begin{pmatrix} m\mathbf{r}_{\mathrm{S}}'' \\ \boldsymbol{\Theta}_{\mathrm{S}}\boldsymbol{\omega}_{\mathrm{S}}' + \widetilde{\boldsymbol{\omega}}_{\mathrm{S}}\boldsymbol{\Theta}_{\mathrm{S}}\boldsymbol{\omega}_{\mathrm{S}} \end{pmatrix}}_{\mathbf{b}_{\mathrm{S}}(s)} z + \underbrace{\begin{pmatrix} m\mathbf{g} \\ \mathbf{0} \end{pmatrix}}_{\mathbf{c}_{\mathrm{S}}(s)} = \mathbf{h}_{\mathrm{S}}. \tag{18}$$

C. EE Wrenches for stable Grasp

The effective net wrench $\mathbf{h}_{\mathrm{S}}$ at the COM must be distributed among the two EEs. Denote with $\mathbf{h}_{\mathrm{SE12}} = (\mathbf{f}_{\mathrm{SE1}}^T, \mathbf{m}_{\mathrm{SE1}}^T, \mathbf{f}_{\mathrm{SE2}}^T, \mathbf{m}_{\mathrm{SE2}}^T)^T$ the overall vector of EE forces and torques that generate the net wrench, i.e. $\mathbf{h}_{\mathrm{S}} = \mathbf{W}\mathbf{h}_{\mathrm{SE12}}$ according to (11), but do not produce an internal grasp wrench. These are determined by the pseudoinverse solution

in (12) as $\mathbf{h}_{\mathrm{E}12} = \mathbf{W}^{\#}\mathbf{h}_{\mathrm{S}}$. Written separately, the forces and torques at the respective EE are

$$\mathbf{f}_{\mathrm{SE}1} = \mathbf{f}_{\mathrm{SE}2} = \frac{1}{2}\mathbf{f}_{\mathrm{S}} \tag{19}$$

$$\mathbf{m}_{\mathrm{SE}i} = \mathbf{m}_{\mathrm{SE}i} = \frac{1}{2}\left(\mathbf{m}_{\mathrm{S}} - \widetilde{\mathbf{r}}_{\mathrm{SE}i}\mathbf{f}_{\mathrm{S}}\right),\ i = 1, 2. \tag{20}$$

This corresponds to an equal distribution among the EEs, which is due to the weighting matrix $\mathbf{G}$ in (13). A different distribution can be achieved using another weighting matrix, if desired. The solution (19) does not generate internal prestressing. In order to ensure a stable grasp by the unilateral grasp contact, additional EE wrenches are required (which must be generated by the admittance control), which do not produce a net wrench. These additional forces/torques are summarized in $\mathbf{h}_{\mathrm{IE}12} = (\mathbf{f}_{\mathrm{IE}1}^T, \mathbf{m}_{\mathrm{IE}1}^T, \mathbf{f}_{\mathrm{IE}2}^T, \mathbf{m}_{\mathrm{IE}2}^T)^T$. Let $\mathbf{h}_{\mathrm{I}} = (\mathbf{f}_{\mathrm{I}}^T, \mathbf{m}_{\mathrm{I}}^T)^T$ be the grasp wrench according to the desired internal prestressing. The required EE wrenches are determined by the null-space component in the solution (12) as $\mathbf{h}_{\mathrm{IE}12} = \mathbf{V}\mathbf{h}_{\mathrm{I}}$, i.e.

$$\begin{aligned} \mathbf{f}_{\mathrm{IE}1} &= -\mathbf{f}_{\mathrm{I}},\ \mathbf{f}_{\mathrm{IE}2} = \mathbf{f}_{\mathrm{I}} \\ \mathbf{m}_{\mathrm{IE}1} &= -\mathbf{m}_{\mathrm{I}} + \widetilde{\mathbf{r}}_{\mathrm{SE}1}\mathbf{f}_{\mathrm{I}},\ \mathbf{m}_{\mathrm{IE}2} = \mathbf{m}_{\mathrm{I}} - \widetilde{\mathbf{r}}_{\mathrm{SE}2}\mathbf{f}_{\mathrm{I}}. \end{aligned} \tag{21}$$

The overall EE wrenches are thus

$$\mathbf{h}_{\mathrm{E}i} = \begin{pmatrix} \mathbf{f}_{\mathrm{SE}i} + \mathbf{f}_{\mathrm{IE}i} \\ \mathbf{m}_{\mathrm{SE}i} + \mathbf{m}_{\mathrm{IE}i} \end{pmatrix},\ i = 1, 2. \tag{22}$$

Usually, no internal grasp torque is desired, i.e. $\mathbf{m}_{\mathrm{I}} = \mathbf{0}$.

The solution (19) for the EE wrenches $\mathbf{h}_{\mathrm{SE}i}$, which generate the net wrench $\mathbf{h}_{\mathrm{S}}$ to move the object, is obtained from the wrench balance assuming that both EEs are fixed to the object, and does hence not take into account the unilateral nature of the grasp contact. As a consequence, the solution (19) may lead to a contact force $\mathbf{f}_{\mathrm{SE}i}$ at EE i pulling away from the object. Therefore, the motion planning must ensure that the contact force normal to the object surface is within a certain range dictated by friction cone (see (27) below).

Denote with $\mathbf{J}_i$ the forward kinematics Jacobian of robot $i = 1, 2$. The generalized drive forces are determined as

$$\mathbf{Q}_{\mathrm{E}i} = \mathbf{J}_i^T\mathbf{h}_{\mathrm{E}i} = \mathbf{a}_{\mathrm{E}i}z' + \mathbf{b}_{\mathrm{E}i}z + \mathbf{c}_{\mathrm{E}i},\ i = 1, 2 \tag{23}$$

with

$$\mathbf{a}_{\mathrm{E}i} := \mathbf{J}_i^T\mathbf{a}_{\mathrm{S}i},\quad \mathbf{b}_{\mathrm{E}i} := \mathbf{J}_i^T\mathbf{b}_{\mathrm{S}i},\quad \mathbf{c}_{\mathrm{E}i} := \mathbf{J}_i^T\mathbf{c}_{\mathrm{S}i}. \tag{24}$$

The pose of EE frame $i = 1, 2$ is described by the position vector $\mathbf{r}_{\mathrm{E},i}$ from the world-fixed inertial frame to the origin of EE frame i, and by the rotation matrix $\mathbf{R}_{\mathrm{IE},i}$ from the EE frame to the inertial frame (see Sec. II. During the grasp, the pose of the EE of robot $i = 1, 2$ can be computed from the pose of the object (15) together with the vectors $\mathbf{r}_{\mathrm{SE}1}$ and $\mathbf{r}_{\mathrm{SE}2}$ (see Sec. V-B).

It is assumed w.l.o.g. that the respective EE frame is oriented such that its x-axis is aligned with the surface normal (pointing away from the body). Then the penetration Δx is the x-component of the deviation of the desired EE pose (corresponding to $\mathbf{q}_{\mathrm{d}}$) from the controlled EE pose (corresponding to $\mathbf{q}_{\mathrm{c}}$), i.e. $\Delta\mathbf{z}_{\mathrm{E}}^T = ((\Delta x, 0, 0)^T, \mathbf{0}^T)$.The EE forces $\mathbf{f}_{\mathrm{E}i}$ are expressed in the inertial frame. Denote with $\mathbf{R}_{\mathrm{SE},i}$ the rotation matrix from the EE frame $i = 1, 2$ to the COM frame of the object. The normal force, and the tangential forces (components along the x- axis^, and the y- and z-axis of the EE-frame, respectively) are

$$\begin{aligned} f_{\mathrm{N},i} &= (\ 1\ 0\ 0\ )\,\mathbf{R}_{\mathrm{SE},i}\mathbf{R}_{\mathrm{IE},i}^T\mathbf{f}_{\mathrm{E}i} = a_{\mathrm{N},i}z' + b_{\mathrm{N},i}z + c_{\mathrm{N},i} \\ f_{\mathrm{T}1,i} &= (\ 0\ 1\ 0\ )\,\mathbf{R}_{\mathrm{SE},i}\mathbf{R}_{\mathrm{IE},i}^T\mathbf{f}_{\mathrm{E}i} = a_{\mathrm{T}1,i}z' + b_{\mathrm{T}1,i}z + c_{\mathrm{T}1,i} \\ f_{\mathrm{T}2,i} &= (\ 0\ 0\ 1\ )\,\mathbf{R}_{\mathrm{SE},i}\mathbf{R}_{\mathrm{IE},i}^T\mathbf{f}_{\mathrm{E}i} = a_{\mathrm{T}2,i}z' + b_{\mathrm{T}2,i}z + c_{\mathrm{T}2,i} \end{aligned} \tag{25}$$

where $a_{\mathrm{N},i} := (\ 1\ 0\ 0\ )\,\mathbf{R}_{\mathrm{EI},i}\mathbf{a}_{\mathrm{E},i}$ etc. are defined by incorporating (23).

The cooperative grasp is stable if the tangential force satisfies

$$f_{\mathrm{T},i} = \sqrt{f_{\mathrm{T}1,i}^2 + f_{\mathrm{T}2,i}^2} \le \mu f_{\mathrm{N},i} \tag{26}$$

where μ is the coefficient of friction. This non-slipping condition (static friction) is translated into two inequality conditions. The first condition

$$0 < \underline{f}_{\mathrm{N},i} \le a_{\mathrm{N}i}z' + b_{\mathrm{N}i}z + c_{\mathrm{N}i} \le \overline{f}_{\mathrm{N},i} \tag{27}$$

ensures that the normal force is positive and between the (positive) limits $\underline{f}_{\mathrm{N},i}$ and $\overline{f}_{\mathrm{N},i}$. If (27) is satisfied, i.e. $f_{\mathrm{N},i}$ is positive, both sides of the condition (26) can be squared

$$f_{\mathrm{T}1,i}^2 + f_{\mathrm{T}2,i}^2 \le \mu f_{\mathrm{N},i}^2. \tag{28}$$

Inserting the relations (25), yields for EE $i = 1, 2$

$$a_{\mu,i}z'^2 + (b_{\mu1,i} + b_{\mu2,i})\,z' + c_{\mu1,i}z^2 + c_{\mu2,i}z + c_{\mu3,i} \le 0 \tag{29}$$

with

$$\begin{aligned} a_{\mu,i} &:= a_{\mathrm{T}1,i}^2 + a_{\mathrm{T}2,i}^2 - \mu^2 a_{\mathrm{N}i}^2 \\ b_{\mu1,i} &:= 2\left(a_{\mathrm{T}1,i}b_{\mathrm{T}1,i} + a_{\mathrm{T}2,i}b_{\mathrm{T}2,i} - \mu^2 a_{\mathrm{N}i}b_{\mathrm{N}i}\right) \\ b_{\mu2,i} &:= 2\left(a_{\mathrm{T}1,i}c_{\mathrm{T}1,i} + a_{\mathrm{T}2,i}c_{\mathrm{T}2,i} - \mu^2 a_{\mathrm{N}i}c_{\mathrm{N}i}\right) \\ c_{\mu1,i} &:= b_{\mathrm{T}1,i}^2 + b_{\mathrm{T}2,i}^2 - \mu^2 b_{\mathrm{N}i}^2 \\ c_{\mu2,i} &:= 2\left(b_{\mathrm{T}1,i}c_{\mathrm{T}1,i} + b_{\mathrm{T}2,i}c_{\mathrm{T}2,i} - \mu^2 b_{\mathrm{N}i}c_{\mathrm{N}i}\right) \\ c_{\mu3,i} &:= c_{\mathrm{T}1,i}^2 + c_{\mathrm{T}2,i}^2 - \mu^2 c_{\mathrm{N}i}^2. \end{aligned}$$

The conditions (27) and (29) can be evaluated for a given object trajectory $\mathbf{r}_{\mathrm{S}}(s), \mathbf{R}_{\mathrm{IS}}(s)$, parameterized by the curve parameter $s(t)$, and be used within the trajectory planning as described in the next section.

V. Time Optimal Path Following for Admittance Controlled Cooperative Grasping

A. Problem Formulation

In case of optimal path following, the desired motion path (position and orientation) of the object is prescribed as in (15). Denote with $\mathbf{q}_1$ and $\mathbf{q}_2$ the joint coordinate vector of robot 1 and 2, respectively. The task is to determine the object trajectory along the prescribed path, i.e. $s(t)$, and the corresponding trajectories of the robots, i.e. $\mathbf{q}_1(t)$ and $\mathbf{q}_2(t)$, which minimize the task duration t_e while ensuring stability of the cooperative grasp and respecting the technological limits of the robots.

The grasp is achieved by introducing a virtual (constant) penetration Δx of the object by the EE (Fig. 3). The

actual grasp force is a result of the admittance, i.e. of the (controlled) compliance. The penetration Δx must be such that the resulting normal force $f_{\mathrm{N},i}$ satisfies the friction cone condition (28) at any time, noting that the tangential forces $f_{\mathrm{T1},i}, f_{\mathrm{T2},i}$ depend on the motion of the object (see Sec. V.C).

For the trajectory planning it is assumed that there is no slipping of the object so that the grasp kinematics, i.e. $\mathbf{r}_{\mathrm{SE1}}$ and $\mathbf{r}_{\mathrm{SE2}}$ in Fig. 2, are constant. It is further assumed that neither the robots nor the object contacts with the environment; consequently spatial admittance is not regulated.

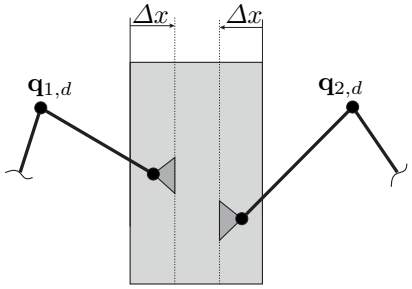

Fig. 3. Commanded (virtual) penetration to generate desired wrench.

B. Inverse Kinematics for given Object Trajectory

For given trajectory of the object, and thus of the two EE, the joint trajectories $\mathbf{q}_1(t)$ and $\mathbf{q}_2(t)$ are computed by solving the inverse kinematics problem. The EE trajectory is expressed in terms of the path parameter $s(t)$, as in (15), and with the inverse kinematics solution, also the joint trajectories are expressed in terms of $s(t)$, as in (2). For a kinematically non-redundant serial robot, starting at a known initial pose, a unique inverse kinematics solution can be computed as long as it does not pass through a singularity. The inverse kinematics problem of robot $i = 1, 2$ is solved by time integration of $\dot{\mathbf{q}}_i = \mathbf{J}_i^{-1}\mathbf{V}_{\mathrm{E}}$. The EE twist $\mathbf{V}_{\mathrm{E}}$ is known from the prescribed motion of the object [13]. Therewith, the motion $\mathbf{q}_i(t)$ of robot $i = 1, 2$ is known.

In case of admittance controlled collaborative grasping, the grasp wrench is indirectly controlled via the admittance by prescribing a virtual penetration Δx (Fig. 3). Therefore, the EE motion of robot $i = 1, 2$ is determined from the prescribed motion of the object, and the penetration Δx is used as an offset to the respective position $\mathbf{r}_{\mathrm{E},i}$. The inverse kinematics of robot $i = 1, 2$ is then solved using these EE poses. The object trajectory leading to minimal time motion is determined in the next section.

C. Solution using Dynamic Programing

The time optimal control problem consists in finding the smallest end time t_e. The latter can be determined from the speed $\sqrt{z}$ along the path as $t_e = \int_0^1 \frac{ds}{\sqrt{z}}$. The path parameter $s(t)$ is normalized such that $s(t_0) = 0$ at the begin and $s(t_e) = 1$ at the end of the path.

The trajectory planning aims at minimum time motion, but at the same time it must respect technological limits of the robots. In particular, requirements on the continuity of the trajectory and the drive torques are crucial in order to achieve trajectories that are actually applicable to the real system [10]. The technological limits of the robots are described by the minimal/maximal joint velocity $\underline{\dot{\mathbf{q}}}, \overline{\dot{\mathbf{q}}}$, acceleration $\underline{\ddot{\mathbf{q}}}, \overline{\ddot{\mathbf{q}}}$, and jerk $\underline{\dddot{\mathbf{q}}}, \overline{\dddot{\mathbf{q}}}$, the minimal/maximal drive torques $\underline{\mathbf{Q}}, \overline{\mathbf{Q}}$. Power constraints can be defined for single motors as well as for the overall power of the robotic system. The latter account for the limits of the electrical power converter. Such limits are considered here, where $\underline{P}_m$ and $\overline{P}_m$ are the minimal and maximal power limits that can be transferred by the power converter. Notice that, in correspondence with the motor characteristics, the motor torque limits $\underline{\mathbf{Q}}, \overline{\mathbf{Q}}$ are velocity dependent. Together with the non-slipping constraints (28), (29), the time optimal path following problem is expressed as follows

$$t_e = \int_0^1 \frac{ds}{\sqrt{z}} \rightarrow \min_{z(s)} \tag{30}$$

$$q_k'^2 z \leq \overline{\dot{q}}_k^2, k = 1, \ldots, n \tag{31}$$

$$\underline{\ddot{\mathbf{q}}} \leq \mathbf{q}'' z + \frac{1}{2}\mathbf{q}' z' \leq \overline{\ddot{\mathbf{q}}} \tag{32}$$

$$\underline{\dddot{\mathbf{q}}} \leq \left(\mathbf{q}''' z + \frac{3}{2}\mathbf{q}'' z' + \frac{1}{2}\mathbf{q}' z''\right)\sqrt{z} \leq \overline{\dddot{\mathbf{q}}} \tag{33}$$

$$\underline{\mathbf{Q}}(\dot{\mathbf{q}}) \leq \mathbf{a}z' + \mathbf{b}z + \mathbf{c} + \mathbf{d}\sqrt{z} \leq \overline{\mathbf{Q}}(\dot{\mathbf{q}}) \tag{34}$$

$$\underline{P}_m \leq (\mathbf{a}z' + \mathbf{b}z + \mathbf{c} + \mathbf{d}\sqrt{z})^T \mathbf{q}'\sqrt{z} \leq \overline{P}_m \tag{35}$$

$$\underline{f}_{\mathrm{N},i} \leq a_{\mathrm{N}i}z' + b_{\mathrm{N}i}z + c_{\mathrm{N}i} \leq \overline{f}_{\mathrm{N},i} \tag{36}$$

$$a_{\mu,i}z'^2 + (b_{\mu 1,i} + b_{\mu 2,i})z' + c_{\mu 1,i}z^2 + c_{\mu 2,i}z + c_{\mu 3,i} \leq 0 \tag{37}$$

where (31)-(37) are formulated for both robots 1 and 2 (index is omitted for sake of simplicity). The inequality constraints (31), (32), (33) restrict the joint velocity, acceleration, and jerk; (34) limits the actuation torques, and (35) is a bound on the overall power. The inequalities (36) and (37) impose the limits on the EE wrenches required to hold the object in order to ensure a stable grasp.

Various methods for the numerical solution of optimal motion planning and time optimal path following in particular have been proposed. Besides application of general purpose multiple shooting methods [21], the numerical integration [2], [16], [17], and the dynamic programming methods [10], [18] were proposed. While being generally applicable, the multiple shooting method is computationally expensive. Numerical integration and dynamic programing on the other hand were identified as well suited for optimal trajectory planning. Until recently, for both methods it was problematic to incorporate third-order constraints, i.e. limits on the jerk along with constraints on velocities and accelerations. A dynamic programming method that allows respecting third-order constraints has been proposed in [10]. Recently also a formulation of the numerical integration method was reported in [16] which accounts for third-order constraints. In [13] third-order constraints were incorporated by piecewise linear interpolation of z. The dynamic programing is deemed advantageous because of its better computational performance, and because the results of [16],[13] must still be interpolated in order to actually achieve smooth jerks.

When using admittance control, the prescribed virtual penetration Δx is crucial to ensure stable grasping. A solution of the optimal control problem satisfies the grasp conditions,

i.e. the constraints (36),(37), so that the maximally required normal (grasping) force never exceeds $\overline{f}_{\mathrm{N},i}$. The penetration Δx is thus determined by the desired EE-stiffness in (6), i.e. the k_1 entry of the diagonal matrix $\mathbf{K}_{\mathrm{E}} = \mathrm{diag}(k_1, \ldots, k_6)$. Setting $\Delta x = \overline{f}_{\mathrm{N}} k_1$ generates the required normal force. While the so determined penetration ideally produces the desired force, it will be shown in the next section that the admittance dynamics has an effect for highly dynamic motions.

VI. Experimental Results

The proposed time optimal admittance control scheme was implemented on a testbed consisting of two 6DOF Comau Racer 3 robots (Fig. 4). Both robots are controlled by B&R Industrial Automation power electronics and industrial PC allowing for real time access to all control variables and measurement signals in a cycle time of 400μs. The reach in workspace is about 0.7 m and the maximum payload is 3 kg each. Both robots are equipped with JR3 multi-axis force-torque sensors (model 67M25A3). The desired admittance is determined by the matrices $\mathbf{M}_{\mathrm{E}}, \mathbf{K}_{\mathrm{E}}$, and $\mathbf{D}_{\mathrm{E}}$ in (6). Their particular choice determines the 'admittance dynamics' in task space, and they must be chosen so to ensure stability. Moreover, since the mass matrix $\boldsymbol{\Lambda}$ in (5) collocated at the EE is configuration dependent and may differ significantly from the desired task space mass matrix, it is reasonable to make $\mathbf{M}_{\mathrm{E}}$ configuration dependent also. It was shown in [9] that the following setting avoids oscillations

$$\mathbf{M}_{\mathrm{E}} = k_M \mathrm{diag}\,(m_1, \ldots, m_6) := k_M \mathrm{diag}\,(\boldsymbol{\Lambda}) \tag{38}$$

$$\mathbf{K}_{\mathrm{E}} := \mathrm{diag}\,(k_1, \ldots, k_6)\,,\ \mathbf{D}_{\mathrm{E}} := \mathrm{diag}\,(d_1, \ldots, d_6) \tag{39}$$

where $\mathrm{diag}\,(\boldsymbol{\Lambda})$ is the diagonal matrix with the diagonal elements $m_1, \ldots, m_6$ of $\boldsymbol{\Lambda}$. The damping coefficients are set to $d_i = 2\xi_i \sqrt{k_i m_i}$ with desired damping ratios ξ_i. The final tuning parameters are thus k_M, k_i, and ξ_i. In the experiment, the parameter values $k_M = 1, \xi_i = 4$, and

$$\mathbf{K}_{\mathrm{E}} = 10^3 \mathrm{diag}\left(10\frac{\mathrm{N}}{\mathrm{m}}, 8\frac{\mathrm{N}}{\mathrm{m}}, 8\frac{\mathrm{N}}{\mathrm{m}}, 0.5\frac{\mathrm{Nm}}{\mathrm{rad}}, 0.5\frac{\mathrm{Nm}}{\mathrm{rad}}, 0.5\frac{\mathrm{Nm}}{\mathrm{rad}}\right).$$

are used. The manipulated object is a solid box with 1.6 kg mass, its COM at the geometric center (Fig. 4), and principal inertia moments $\boldsymbol{\Theta}_{\mathrm{S}} = \mathrm{diag}\ (0.006, 0.002, 0.004)\ \mathrm{kg} \cdot \mathrm{m}^2$.

The time optimal trajectory planning problem was solved with two different limits on the maximal jerk: i) moderate, and ii) high jerk, leading to moderately fast and fast motion,

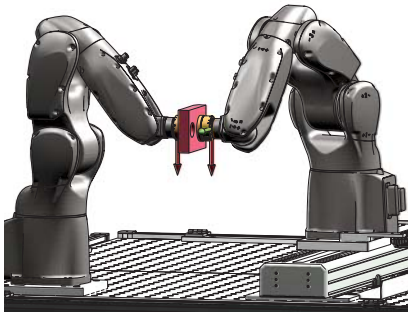

Fig. 4. Experimental setup with two cooperating Comau Racer 3 robots.

respectively. The limits are listed in table I. The minimal values of the limits are set to the negative maximal values, e.g. $\underline{\mathbf{Q}} = -\overline{\mathbf{Q}}$. The bounds for the overall power are $\underline{P}_m = -2$ kW and $\overline{P}_m = 1.2$ kW. The bounds for the normal forces are chosen as $\underline{f}_N = 80$ N and $\overline{f}_N = 120$ N. The friction coefficient is set to $\mu = 0.9 \tan(\rho)$ where the friction angle $\rho = 28°$ was determined experimentally. The virtual penetration was determined as $\Delta x = 12$ mm.

TABLE I
LIMITS USED FOR TRAJECTORY OPTIMIZATION.

axis	$\overline{\dot{\mathbf{q}}}$ [$°/s$]	$\overline{\mathbf{Q}}$ [Nm]	i) $\overline{\dddot{\mathbf{q}}}$ [$°/s^3$]	ii) $\overline{\dddot{\mathbf{q}}}$ [$°/s^3$]
1	396	328	2.5e5	1.44e6
2	405	320	2.5e5	1.44e6
3	450	145	2.5e5	1.44e6
4	540	61	2.5e5	1.44e6
5	540	61	2.5e5	1.44e6
6	810	40	2.5e5	1.44e6

The dynamic programing method reported in [10] (denoted DP3) was used, which accounts for jerk (third-order) constraints. The numerical accuracy and complexity is determined by the number N_{s} of path points, the number N_{z} of points at which the squared path velocity z evaluated at each path point, and the number N_{ch} of checkpoints where the third-order interpolation function is evaluated [10]. In the experiment, $N_{\mathrm{s}} = 102, N_{\mathrm{z}} = 1020, N_{\mathrm{ch}} = 10$ were used.

First consider the motion with moderate jerk limits i) in table I. Fig. 5 shows the grasp forces measured during the experiment. The normal force was always within the desired range of $f_N = 80, \ldots, 120$N. The implemented admittance control achieved a stable (reproducible) grasp of the object.

Next consider the results for high jerk limit, which leads to a highly dynamic grasping scenario. Fig. 6 shows joint velocities $\dot{\mathbf{q}}$, jerks $\dddot{\mathbf{q}}$, and the drive torque Q_3 (all normalized to their maximum values) for robot 1 as a result of solving the optimal control problem (30)-(37). Only drive torque Q_3 is shown due to space limitation. The red lines indicate the limits for the respective values. Since the motor characteristic is taken into account, this bound is not constant. Additionally, the optimization result for the normal force is depicted. None of the limits are violated. Results for the other values as well as for the second robot are similar. Since the motion is time-optimal, always one of the limits is active. The measurement of the actual values are almost identical to the precomputed values, and are not shown here. The measurements of the contact wrench of robot 1 are shown in Fig. 7. Clearly, the normal force f_x frequently violates the minimal and maximal value, and this is similar at the second robot. This can be mainly attributed to the geometric inaccuracies of the robots. The dynamic model parameters of the robots where identified (indispensable for model-based control) but the robots were not calibrated. The positioning precision of the Comau robots was experimentally determined to be in the range below 10mm. The corresponding deviation of the EE motion from its nominal value must be compensated by the admittance control scheme. This works well for moderate speed, but the control scheme cannot fully compensate this error at very high speed. To this end, the parameters in

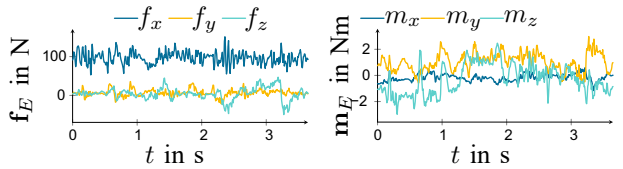

Fig. 5. Measured wrench at EE $i = 1$ during time optimal motion with moderate jerk limit.

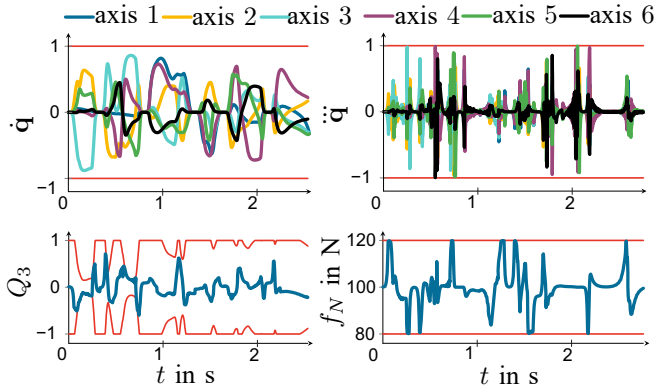

Fig. 6. Joint velocities and jerks, drive torque Q_3 and normal grasp force f_N at EE $i = 1$ as result of the trajectory optimization with high jerk limit.

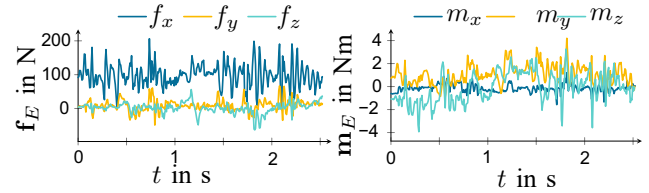

Fig. 7. Measured wrench at EE $i = 1$ during time optimal fast motion.

(10), which determine the admittance dynamics, would need to be adapted. These experimental results reveal the need accurate geometric and dynamic models. Results for both experiments are documented by the video supplement.

VII. Conclusions

The time optimal path following problem of two robots cooperatively grasping an object (in surface contact) was addressed by means of a novel task space admittance control scheme in combination with a recently proposed dynamic programing algorithm which accounts for jerk limits. The jerk limits are important to ensure that the time optimal motions can actually be executed by the robots. The basic idea is to solve the time optimal path following problem with a dynamic programing algorithm, where the EE wrenches are always within predefined limit so to ensure a stable grasp (normal force and according tangential friction forces). The EE wrench is then controlled by means of an admittance control scheme, rather than by direct force or impedance control. To this end, a virtual penetration is defined that, according to the controlled admittance, yields the grasp wrench. The approach was validated experimentally. It was further shown that the selection of virtual penetration is crucial and depends on the dynamics of the grasping motion. Future work will address tuning of the admittance dynamics and the computationally efficient determination of the virtual penetration for a given motion. Extension to cooperating parallel manipulators is envisaged.

VIII. Acknowledgement

This work has been supported by the LCM K2 Center for Symbiotic Mechatronics within the framework of the Austrian COMET-K2 program.

References

[1] S. Arimoto, F. Miyazaki, S. Kawamura: Cooperative motion control of multiple robot arms or fingers. In Proceedings of the 1987 IEEE International Conference on Robotics and Automation (ICRA) 1987, Vol. 4, pp. 1407-1412

[2] J. Bobrow, S. Dubowsky, J. Gibson: Time-Optimal Control of Robotic Manipulators Along Specified Paths, Int. J. Rob. Res., Vol. 4, No. 3, 1985, pp. 3-17

[3] F. Bruni et al.: Experiments of impedance control on an industrial robot manipulator with joint friction. IEEE Int Con. Control Applications, 1996, pp. 205–210

[4] F. Caccavale et. al: Six-DOF Impedance Control of Dual-Arm Cooperative Manipulators. IEEE/ASME Trans. Mechatronics, Vol. 13, No. 5, 2008, pp. 576-586

[5] A. De Luca, R. Mattone: Actuator failure detection and isolation using generalized momenta. IEEE I. Con. Rob. Aut., 2003, pp. 634–639

[6] S. Hayati: Hybrid position/force control of multi-arm cooperating robots, IEEE Int. Conf. Rob. Automat (ICRA), Vol. 3, 1986, pp. 82-89

[7] D. Kaserer, H. Gattringer, A. Müller: Spatial impedance control of two cooperative industrial manipulators. Proc. Appl. Math. Mech. (PAMM), Vol. 16, 2016, 61–62

[8] D. Kaserer, H. Gattringer, A. Müller: A Task Space Admittance Control Algorithm for Safe Human Robot Interaction, Proc. Appl. Math. Mech. (PAMM), Vol. 18, 2018

[9] D. Kaserer, H. Gattringer, A. Müller: Admittance control of a redundant industrial manipulator without using force/torque sensors, 42nd Annual Conference of IEEE Industrial Electronics Society (IECON), Oct. 24-27, 2016, Firenze (Florence), Italy

[10] D. Kaserer, H.Gattringer, A. Müller: Nearly Optimal Path Following With Jerk and Torque Rate Limits Using Dynamic Programming, IEEE Transactions on Robotics, Vol. 35, No 1, 2019, pp. 521 - 528

[11] O. Khatib: A unified approach for motion and force control of robot manipulators: The operational space formulation. IEEE Journal on Robotics and Automation, Vol. 3, No. 1, 1987, pp. 43–53

[12] M. Makarov, et. al: Adaptive Filtering for Robust Proprioceptive Robot Impact Detection Under Model Uncertainties. IEEE/ASME Trans. Mechatronics, Vol. 19, No. 6, 2014, pp. 1917–1928

[13] J. Mattmüller, D. Gisler: Calculating a near time-optimal jerk-constrained trajectory along a specified smooth path, Int. J. Adv. Manuf. Tech., Vol. 45, No. 9, 2009, pp. 1007-1016

[14] S.S. Mirrazavi Salehian, N. Figueroa, A. Billard: A unified framework for coordinated multi-arm motion planning, Int. J. Rob. Res., 2018, pp. 1-28

[15] V. Perdereau, M. Drouin. Hybrid external control for two robot coordinated motion. Robotica, Vol. 14, No. 2, 1996, pp. 141-153

[16] H. Pham, Q. C. Pham: On the structure of the time-optimal path parameterization problem with third-order constraints, IEEE Int. Conf. Rob. Aut., 2017, pp. 679-686

[17] H. Pham, Q. C. Pham: A New Approach to Time-Optimal Path Parameterization Based on Reachability Analysis, IEEE Trans. Rob., Vol. 34, No. 3, pp. 645-659, 2018

[18] F. Pfeiffer, R. Johanni: A Concept for Manipulator Trajectory Planning, IEEE J. Rob. Aut., Vol. 3, No. 2, 1987, pp. 115-123

[19] B. Siciliano und O. Khatib, (Eds.): Handbook of Robotics, Part D, Chapter 39. Springer, 2016

[20] C. Smith, et. al: Dual arm manipulation–A survey, Rob. and Auton. Sys., Vol. 60, No. 10, 2012, pp. 1340-1353

[21] K. Springer, H. Gattringer, P. Staufer: On time-optimal trajectory planning for a flexible link robot, Proc. IMechE Part I: J Systems and Control Engineering, Vol. 227, 2013, pp. 752-763

[22] D. Sun, Y.H. Liu: Position and Force Tracking of a System Manipulating a Flexible Beam, J. Rob. Sys., Vol. 18, 2001, pp. 197-212

[23] D. Sun, Y.H. Liu.: Modeling and impedance control of a two manipulator system handling a flexible beam, IEEE Int. Con. Rob. Aut. (ICRA), 1997, Vol. 2, pp. 1787-792

[24] I. D. Walker, R. A. Freeman, S. I. Marcus. Analysis of Motion and Internal Loading of Objects Grasped by Multiple Cooperating Manipulators. Int. J. Rob. Res., Vol. 10, No. 4, 1991, pp. 396-409